Photon Counting Computed Tomography in Rectal Cancer: Associations Between Iodine Concentration, Histopathology and Treatment Response: A Pilot Study.

Alexey Surov[1], Raihanatou Diallo-Danebrock[1], Amin Radi, Jan Robert Kröger, Julius Henning Niehoff, Arwed Elias Michael, Berthold Gerdes, Saleem Elhabash, Andreas Wienke, Jan Borggrefe

Rationale and Objectives: Common computed tomography (CT) investigation plays a limited role in characterizing and assessing the response of rectal cancer (RC) to neoadjuvant radiochemotherapy (NARC). Photon counting computed tomography (PCCT) improves the imaging quality and can provide multiparametric spectral image information including iodine concentration (IC). Our purpose was to analyze associations between IC and histopathology in RC and to evaluate the role of IC in response prediction to NARC.

Materials and Methods: Overall, 41 patients were included into the study, 14 women and 27 men, mean age, 65.5 years. PCCT in a portal venous phase of the abdomen was performed. In every case, a polygonal region of interest (ROI) was manually drawn on iodine maps. Normalized IC (NIC) was also calculated. Tumor stage, grade, lymphovascular invasion, circumferential resection margin, and tumor markers were analyzed. Tumor regression grade (absence/presence of tumor cells) after NARC was analyzed. NIC values in groups were compared to Mann–Whitney-U tests. Sensitivity, specificity, and area under the curve values were calculated. Intraclass correlation coefficient (ICC) was calculated.

Results: ICC was 0.93, 95%CI = (0.88; 0.96). Tumors with lymphovascular invasion showed higher NIC values in comparison to those without (p = 0.04). Tumors with response grade 2–4 showed higher pretreatment NIC values in comparison to lesions with response grade 0–1 (p = 0.01). A NIC value of 0.36 and higher can predict response grade 2–4 (sensitivity, 73.9%; specificity, 91.7%; area under the curve, 0.85).

Conclusion: NIC values showed an excellent interreader agreement in RC. NIC can predict treatment response to NARC.

Key Words: Photon counting computer tomography; Rectal cancer; Treatment response.

INTRODUCTION

Rectal cancer (RC) is one of the most frequent cancers worldwide (1). Imaging, especially magnetic resonance imaging (MRI) plays an essential role in staging of RC (2,3). Moreover, MRI can also characterize RC. Some reports showed that several MRI features reflect different histopathological findings in RC (2,3). So far apparent diffusion coefficient derived from MRI correlates strongly with the expression of the tumor proliferation marker Ki 67 in RC (2,4). Furthermore, quantitative diffusion kurtosis imaging demonstrates a higher correlation with T-stages and histologic grades (3).

More importantly, imaging can also predict treatment outcome in RC. For instance, it has been shown that apparent

diffusion coefficient correlated with the response rate after neoadjuvant radiochemotherapy (NARC) in RC (5).

Common computed tomography (CT) plays an inferior role in local staging of RC because the spatial resolution and soft tissue contrast is still suboptimal for the pelvic region. However, the introduction of modern CT techniques like photon counting CT (PCCT) significantly improved the imaging of soft tissues (6). Furthermore, PCCT can provide multiparametric spectral image information that conventional CT imaging cannot in this detail and resolution. So far, PCCT has substantial benefits like reduced sensitivity to electronic noise, increased contrast-to-noise ratio, higher spatial resolution, better material decomposition, and higher dose efficiency (7,8). Also PCCT allows the detection, separation, and quantification of iodine contrast agent in solid organs and lesions (7–9). Iodine quantification is defined by iodine concentration (IC) within the analyzed organ or lesion (mg/cm^3) (7–9). According to the literature, IC is an important quantitative parameter (10,11). For example, IC is helpful to differentiate malignant and benign parotid gland lesions (10). Furthermore, IC can better characterize local colonic wall thickening (11).

The purpose of the present study was to analyze possible associations between IC and relevant histopathological features in RC and to evaluate the role of tumoral IC in prediction of response to NARC.

MATERIAL AND METHODS

Study Design, Patients and Tumors

The present retrospective study was approved by the institutional review board (Ethics Committee of the Faculty of Medicine, Ruhr-University Bochum, approval code, 2021–827).

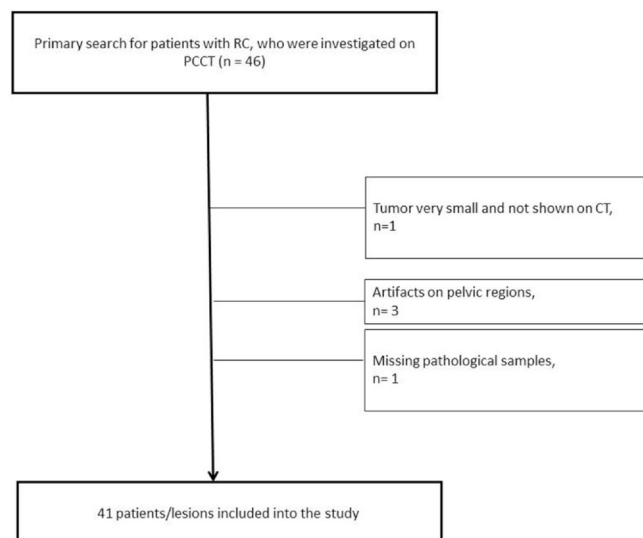For this study, patients with RC, who were investigated on PCCT in our institution in the time period from 01.10.2021 to 31.12.2023 were collected. Figure 1 shows the work flow of the data acquisition.

Inclusion criteria were:

1. primary rectal solid adenocarcinoma;
2. investigation on PCCT;
3. available histopathological specimens
4. available data about treatment response.
   Exclusion criteria were:
5. other tumors than adenocarcinoma: neuroendocrine tumors, mucinous, squamous cell, adenosquamous, spindle cell and undifferentiated carcinomas;
6. significant artifacts on images.

Furthermore, tumor stage (TNM), circumferential resection margin (CRM), serological tumor markers (CEA, carcinoembryonic antigen and CA 19–9) were retrieved from the digital data bank.

PCCT

In all cases, staging examinations included a portal venous CT of the abdomen with the clinically available dual source photon counting CT (NAEOTOM Alpha, software version Syngo CT VA40A/VA50A, Siemens Healthineers, Erlangen, Germany). The examination was performed in the supine position with the arms raised. The tube voltage was 120 kVp, the tube current was modulated based on the manufacturer-specific dose modulation with set image quality level (IQ level) 170. The total collimation was 144 × 0.4 mm, the pitch factor 0.8, the gantry rotation time 0.5 s

For the scan a weight-adjusted (1 mL/kg bodyweight) contrast agent (ACCUPAQUE® 300, GE Healthcare, Chicago, IL, USA) was injected in a peripheral vein of the arm using a coupled automated injector (MEDRAD® Centargo, Bayer Healthcare, Leverkusen, Germany). Injection of the contrast agent at 2.4 mL/s was followed by 40 mL of a NaCl (0.9%) chaser with a flow rate of 2.5 mL/s. Based on density monitoring of a region of interest (ROI) in the descending aorta, the portal venous scan was started 60 s after the threshold of 100 HU was reached in the ROI.

For each scan, a polyenergetic and a spectral data set were reconstructed with the convolution kernels Br36 (polyenergetic) and Qr36 (spectral data sets), respectively, each using the fourth level of iterative reconstruction (Q4, Quantum Iterative Reconstruction, 4 levels of iteration). Virtual monoenergetic images were calculated primarily axially with a slice thickness of 0.6 mm and an increment of 0.4 mm, the matrix was set to 512 × 512.

Imaging Analysis

Analysis of images was performed by two radiologists (SG with 1 years of experience and JHN, board certified radiologist, with 5 years of experience in colorectal imaging), independent to each other and blinded to the
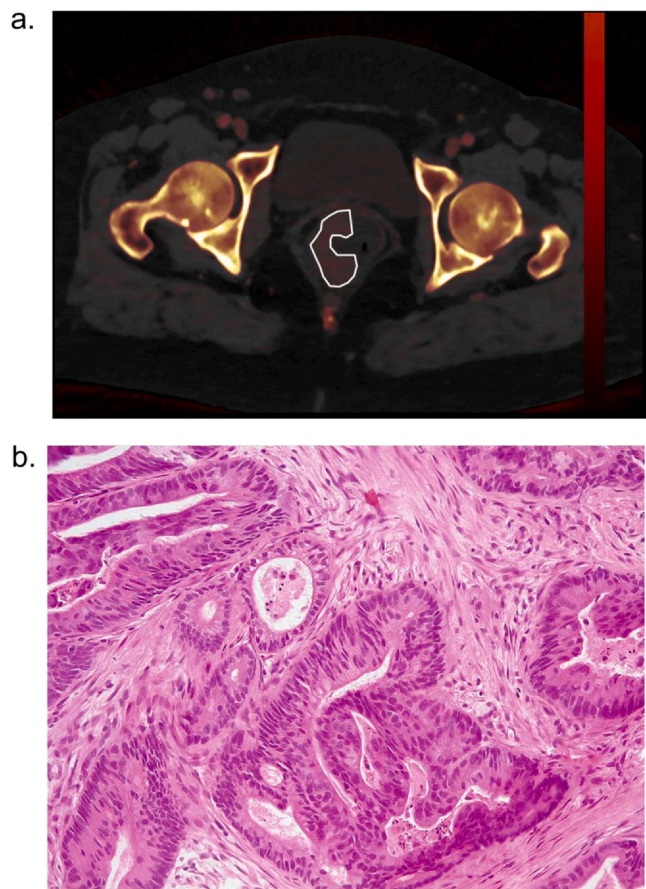

Figure 1. Flow chart of data acquisition.

Figure 2. An example of the study cohort. (**a**) PCCT image (iodine map) documenting a large semicircular rectal tumor with a region of interest around the tumor margins. (**b**) Histopathological image (H&E) showing large rectal cancer deposits.

histopathological findings. The slice with the largest extension of RC was selected and in this image a polygonal region of interest (ROI) as large as possible was manually drawn on iodine maps around the margin of the lesion without risking partial volume effects. For all tumors, mean IC values were estimated (Fig 2a).

At the next step, a round ROI was placed in the abdominal aorta and the IC within the aorta was estimated. Furthermore, normalized IC (NIC) was calculated as a ratio: tumoral IC divided by the IC of the aorta. This approach was performed to reduce technical and/or physiological variabilities in iodine accumulation within the tissue of interest due to varying cardiac output and phase times (12). All analyses were performed on a manufacturer's specific software (Syngo.Via, software version VB60, Siemens Healthineers, Erlangen, Germany).

Histopathological Analysis

The following histopathological features were included into the study and analyzed: tumor grade, affection of lymph vessels, and affection of venous vessels. The analysis was performed on hematoxylin-eosin (H&E) stained images with magnifications of $\times$ 40 and $\times$ 200 (Fig 2b). Furthermore, tumor regression grade after NARC was analyzed according to Dworak et al. (13) as follows: no regression (grade 0), predominantly tumor with significant fibrosis and/or vasculopathy (grade 1), predominantly fibrosis with scattered tumor cells (slightly recognizable histologically) (grade 2), only scattered tumor cells in the space of fibrosis with/without acellular mucin (grade 3), no vital tumor cells detectable (grade 4). All investigations were performed by a board-certified pathologist (RD) with 20 years of clinical experience.

Statistical Analysis

Statistical analysis was performed using the SPSS package (IBM SPSS Statistics for Windows, version 28.0, Armonk, NY, USA: IBM corporation). Continuous variables were described by mean value, median and standard deviation. Categorical variables were given as absolute and relative frequencies. The comparison of NIC values in groups was performed by Mann–Whitney-U tests. The association between NIC and CEA and CA 19–9 values was calculated by Spearman's rank correlation coefficient. Sensitivity, specificity, negative, and positive predictive values, accuracy, and area under the curve values were calculated for the diagnostic procedures. NIC thresholds are chosen to maximize the Youden index. Intraclass correlation coefficients (ICC) were used for calculation of interreader agreement. All p-values were interpreted in an exploratory manner.

RESULTS

Tumor Characteristics and Tumoral NIC

Overall, 41 patients were included into the study. There were 14 women and 27 men with a mean age of 65.5 ± 12.4 years. Tumor and patients characteristics are given in Table 1. In short, most frequently, grade 2 or 3 tumors, in stage T4 with nodal affection were diagnosed. Furthermore, most tumors were without venous or lymphatic vessel invasion. Accordingly, most lesions showed no distant metastases (M0 stage).

The measured NIC values showed an excellent interreader reliability, ICC $= 0.93$, 95%CI $= (0.88; 0.96)$. The mean value of intratumoral NIC was 0.38 ± 0.14, range 0.21–0.90, median value 0.35.

Associations Between NIC and Tumoral Features

NIC had no strong correlations with CEA ($r = 0.12$, $p = 0.46$) and CA 19–9 ($r = 0.08$, $p = 0.68$). There were also no important associations between tumor grade, stage and NIC (Table 2). Tumors with lymphovascular invasion showed higher NIC values in comparison to those without, 0.45 ± 0.17 vs 0.36 ± 0.13 ($p = 0.04$). A NIC value of 0.35 and higher could lymphovascular invasion with a sensitivity of 66.7%, a specificity of 64.7%, a positive predictive value of

TABLE 1. Patients and Tumors

Male	27 (66%)
Female	14 (34%)
Age, M ± SD	65.5 ± 12.4
CEA level, M ± SD	66.4 ± 211.9
CA 19-9 level, M ± SD	392.9 ± 1639.5
T1, n(%)	2 (5%)
T2, n(%)	2 (5%)
T3, n(%)	7 (17%)
T4, n(%)	30 (73%)
N0, n(%)	9 (22%)
N + , n(%)	32 (78%)
M0, n(%)	30 (73%)
M+ , n(%)	11 (27%)
CRM -, n(%)	16 (39%)
CRM+ , n(%)	25 (61%)
Grade 1, n(%)	1 (2%)
Grade 2, n(%)	24 (59%)
Grade 3, n(%)	16 (39%)
L0, n(%)	32 (78%)
L+ , n(%)	9 (22%)
V0, n(%)	38 (93%)
V+ , n(%)	3 (7%)

CEA, carcinoembryonic antigen;

CRM, circumferential resection margin;

L, lymphovascular invasion; M, distant metastases; N, nodal stage;

V, venous vessel invasion

TABLE 2. NIC Values (Mean Values ± Standard Deviation) in RC with Different Histopathological Features

Grade 1/2	Grade 3	p-value
0.36 ± 0.13	0.42 ± 0.15	0.08
CRM+	**CRM-**	
0.38 ± 0.14	0.38 ± 0.15	0.72
N0	**N+**	
0.36 ± 0.09	0.38 ± 0.15	0.96
M0	**M+**	
0.39 ± 0.16	0.36 ± 0.07	0.92
L0	**L+**	
0.36 ± 0.13	0.45 ± 0.17	0.04
V0	**V+**	
0.38 ± 0.15	0.37 ± 0.09	0.80

CRM, circumferential resection margin;

L, lymphovascular invasion; M, distant metastases; N, nodal stage; NIC, normalized iodine concentration; V, venous vessel invasion.

33.3%, a negative predictive value of 87.0%, an area under the curve of 0.73 (Fig 3).

NIC and Treatment Response to NARC

Data about treatment response to NARC were available for 35 patients. In three patients, primary surgical resection
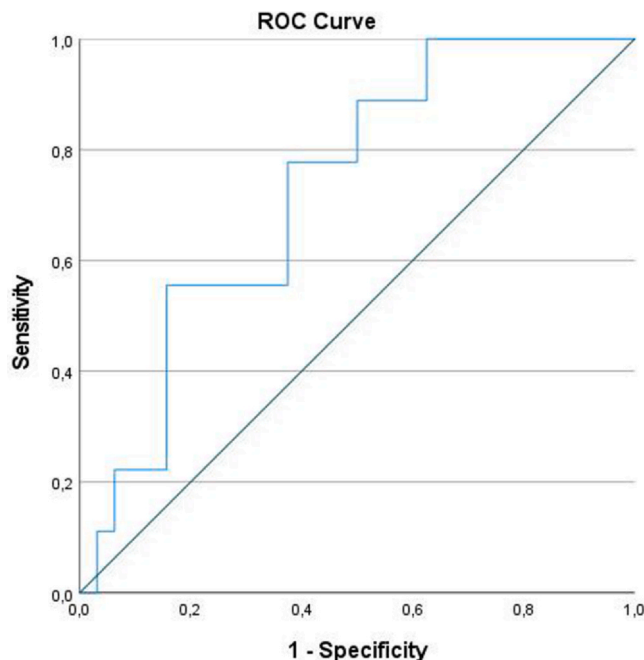

Figure 3. Receiver operating characteristic curve for discrimination of RC with and without lymphovascular invasion. AUC = 0.73, 95%CI = (0.56; 0.90).

without NARC was performed. Two patients died and in one patient the data were not available. NARC included short-course radiotherapy (5×5 Gy over a maximum of 8 days) followed by six cycles of CAPOX chemotherapy (capecitabine 1000 mg/m² orally twice daily on days 1–14, oxaliplatin 130 mg/m² intravenously on day 1, and a chemotherapy-free interval between days 15 and 21) or nine cycles of FOLFOX4 (oxaliplatin 85 mg/m² intravenously on day 1, leucovorin 200 mg/m² intravenously on days 1 and 2, followed by bolus fluorouracil 400 mg/m² intravenously and fluorouracil 600 mg/m² intravenously for 22 h on days 1 and 2, and a chemotherapy-free interval between days 3 and 14) (14).

Treatment response after NARC was as follows: grade 0 ($n = 5$, 14.3%), grade 1 ($n = 7$, 20.0%), grade 2 ($n = 11$, 31.4%), grade 3 ($n = 7$, 20.0%), and grade 4 ($n = 5$, 14.3%).

Tumors with good (response grade 3–4) and moderate (response grade 2) treatment response showed higher pre-treatment NIC values in comparison to lesions with poor response (response grade 0 and 1), 0.44 ± 0.16 vs 0.30 ± 0.06, respectively, p = 0.01 (Fig 4). Furthermore, a NIC cut off was identified for the discrimination of tumors with good/moderate and poor response. A NIC value of 0.36 and higher can predict good/moderate response (response grade 2–4) with a sensitivity of 73.9%, a specificity of 91.7%, a positive predictive value of 94.4%, a negative predictive value of 64.7%, an area under the curve of 0.85, and an accuracy of 80% (Fig 5). Regression analysis showed that this cut off value had an odds ratio of 31.2, 95%CI = (3.3; 295.3), p < 0.01, for prediction of a good/moderate response.
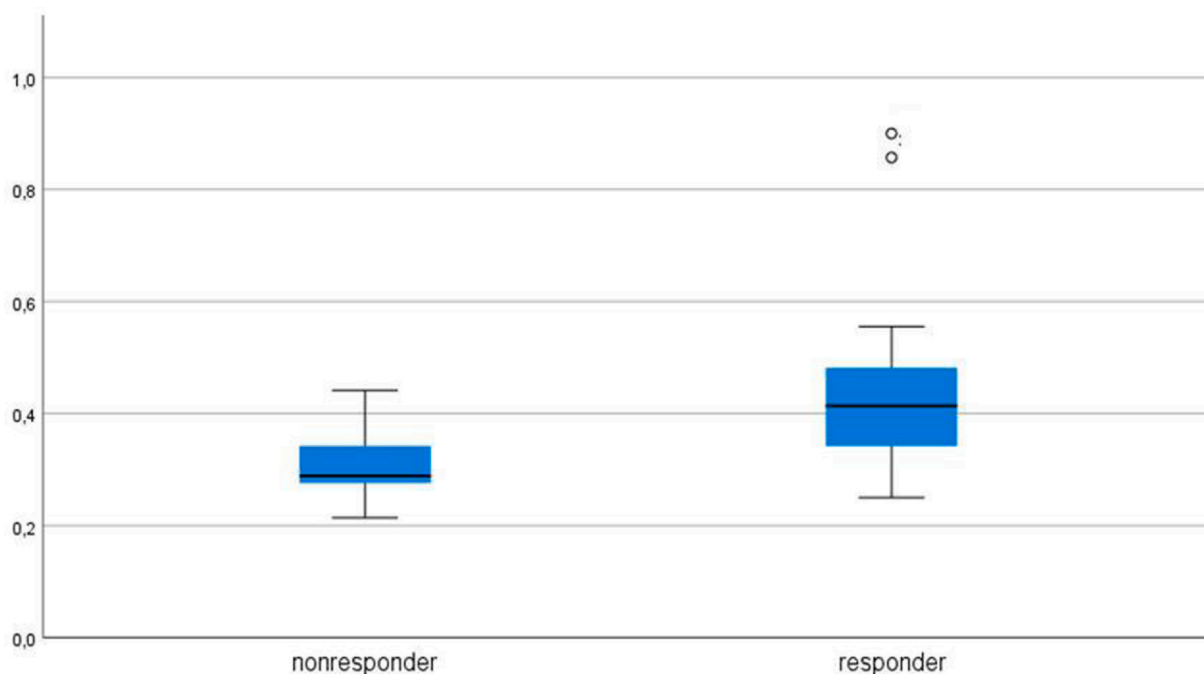
Figure 4. Comparison of normalized iodine concentration values between tumors with good and poor response to neoadjuvant radio-chemotherapy.
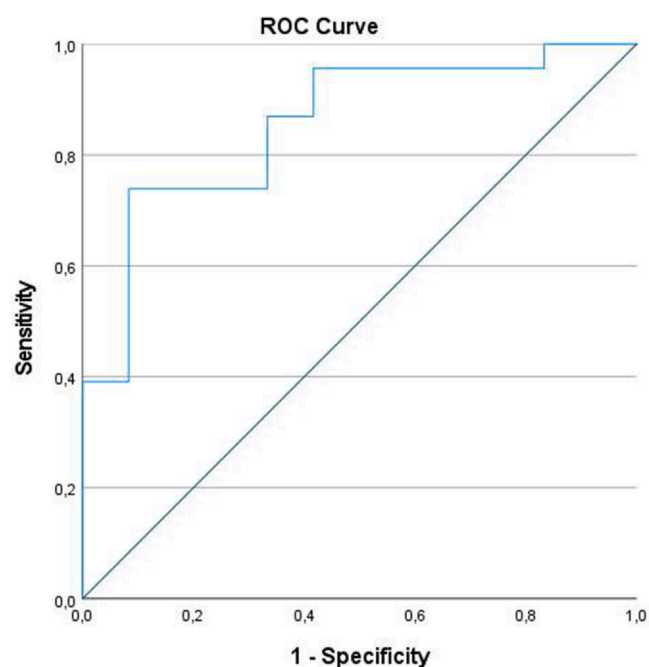

Figure 5. Receiver operating characteristic curve for discrimination of RC with good and poor response to neoadjuvant radio-chemotherapy, AUC = 0.85, CI95% = (0.73;0.99).

DISCUSSION

The present study is the first investigation about the prognostic role of IC on PCCT in RC. We identified that NIC is a robust imaging parameter. Moreover, it can be used for prediction of treatment response in RC.

Previously, some studies analyzed relationships between different histopathological features and IC in several tumors (15–17). In all cases, dual energy CT examinations were performed. For instance, Wang et al. demonstrated that in breast cancer, IC was different between cancer subtypes according to the hormone receptor status (15). In lung cancer, IC can discriminate tumors with high and low expression of the proliferation index Ki 67 (16). Finally, in gastric cancer, IC correlated with microvessel density (17). In RC, only few studies evaluated associations between histopathology and IC or NIC (18–20). Wang et al. identified that IC moderately correlated with Ki 67 in RC (18). In another study, it was shown that NIC can predict extramural vascular invasion (19). According to Fan et al., NIC correlated moderately with expression of hypoxia inducible factor 1a (20).

In the present study, NIC did not correlate with CEA and CA 19–9 levels. Also, NIC did not reflect tumor grade, N and M stages in RC. Furthermore, NIC did not correlate with CRM. Interestingly, NIC correlated with lymphovascular invasion. The exact cause of this finding is unclear. We hypothesize that it may be related to the fact that tumors with lymphovasucular invasion may have a more aggressive pattern with a higher microvessel density. Independently of possible pathophysiological explanations, this finding is very important. In fact, it is well known that the presence of lymphovascular invasion is negatively associated with response to NARC in RC (21). Also RC with lymphovascular invasion is associated

with poorer disease-free and overall survival (22). Therefore, imaging-based prediction of lymphovascular invasion can be beneficial for patients. Although, the identified sensitivity and specificity values are not high, NIC may be used in the clinical routine as an additional predictive tool.

More remarkably, our study showed that NIC can predict response to NARC in RC. This finding is very important for the clinical routine. The ability to identify patients with good response prior to treatment could optimize and personalize management of patient with RC. Moreover, the identified threshold of NIC shows a higher sensitivity/specificity than those of other imaging parameters such as apparent diffusion coefficient (23,24). For instance, in the study of Chen et al. apparent diffusion coefficient showed a sensitivity of 60%, and a specificity of 64% in this regard (23). Furthermore, for the diffusion kurtosis imaging, the reported sensitivity and specificity for positive treatment outcome were 66.7% and 77.8%, respectively (24). Importantly, in contrast to other methods, NIC can be obtained routinely without additional time-consuming investigations and/or post-processing analyses.

Presumably, IC may reflect tumor microvascular density and permeability. Previous investigations showed that hypervascularized RC had a better response to NARC than hypovascularized tumors (25,26). So far, it has been shown that RC with high tumoral blood flow showed better responses to NARC than tumors with low blood perfusion (25). This phenomenon might be explained by some histopathological features. Well-differentiated tumors host mature vessels with near-regular endothelial walls and patent lumens. More mature vessels can permit a higher exchange between the blood bed and the interstitial space, with more effective passage and permeability of different substances, including contrast media (27). In contrast, poorly differentiated tumors consist of disorganized and leaky vessels, with ineffective exchange and inefficient delivery of substances (27).

The present study has some limitations. First, it is retrospective. Second, our results are based on a small number of patients. Clearly, further analyses are needed to proof our promising results.

In conclusion, NIC values showed an excellent inter-reader variability in RC. Tumoral NIC may be helpful for prediction of lymphovascular invasion. NIC can predict treatment response to NARC. Therefore, NIC can be used as a novel imaging biomarker in RC.

ETHICAL APPROVAL

Institutional Review Board approval was obtained.

COMPLIANCE WITH ETHICAL STANDARDS

Guarantor:

The scientific guarantor of this publication is professor Surov.

STATISTICS AND BIOMETRY

One of the authors has significant statistical expertise.

INFORMED CONSENT

Written informed consent was waived by the Institutional Review Board.

STUDY SUBJECTS OR COHORTS OVERLAP

None.

METHODOLOGY

Methodology:

- retrospective
- case-control study
- observational
- performed at one institution

REFERENCES

1. Siegel RL, Miller KD, Goding Sauer A, et al. Colorectal cancer statistics, 2020. CA Cancer J Clin 2020; 70(3):145–164.
2. Ao W, Bao X, Mao G, et al. Value of apparent diffusion coefficient for assessing preoperative T staging of low rectal cancer and whether this is correlated with Ki-67 expression. Can Assoc Radiol J 2020; 71(1):5–11.
3. Yuan J, Gong Z, Liu K, et al. Correlation between diffusion kurtosis and intravoxel incoherent motion derived (IVIM) parameters and tumor tissue composition in rectal cancer: a pilot study. Abdom Radiol (NY) 2022; 47(4):1223–1231.
4. Surov A, Pech M, Powerski M, et al. Pretreatment apparent diffusion coefficient cannot predict histopathological features and response to neoadjuvant radiochemotherapy in rectal cancer: a meta-analysis. Dig Dis 2022; 40(1):33–49.
5. Delli Pizzi A, Cianci R, Genovesi D, et al. Performance of diffusion-weighted magnetic resonance imaging at 3.0T for early assessment of tumor response in locally advanced rectal cancer treated with preoperative chemoradiation therapy. Abdom Radiol (NY) 2018; 43(9):2221–2230.

6. Wu Y, Ye Z, Chen J, et al. Photon counting CT: technical principles, clinical applications, and future prospects. Acad Radiol 2023; 30(10):2362–2382.

7. Wrazidlo R, Walder L, Estler A, et al. Radiation dose reduction in contrast-enhanced abdominal CT: comparison of photon-counting detector CT with 2nd generation dual-source dual-energy CT in an oncologic cohort. Acad Radiol 2023; 30(5):855–862.

8. Sartoretti T, Mergen V, Jungblut L, et al. Liver iodine quantification with photon-counting detector CT: accuracy in an abdominal phantom and feasibility in patients. Acad Radiol 2023; 30(3):461–469.

9. Vrbaski S, Bache S, Rajagopal J, et al. Quantitative performance of photon-counting CT at low dose: Virtual monochromatic imaging and iodine quantification. Med Phys 2023; 50(9):5421–5433.

10. Wang Y, Hu H, Ban X, et al. Evaluation of quantitative dual-energy computed tomography parameters for differentiation of parotid gland tumors. Acad Radiol 2023(23):S1076–6332. 00444-0.

11. Wang G, Fang Y, Wang Z, et al. Quantitative assessment of radiologically indeterminate local colonic wall thickening on iodine density images using dual-layer spectral detector CT. Acad Radiol 2021; 28(10):1368–1374.

12. Tian S, Jianguo X, Tian W, et al. Application of dual-energy computed tomography in preoperative evaluation of Ki-67 expression levels in solid non-small cell lung cancer. Med (Baltimore) 2022; 101(31):e29444.

13. Thies S, Langer R. Tumor regression grading of gastrointestinal carcinomas after neoadjuvant treatment. Front Oncol 2013; 3:262.

14. Bahadoer RR, Dijkstra EA, van Etten B, et al. RAPIDO collaborative investigators. Short-course radiotherapy followed by chemotherapy before total mesorectal excision (TME) versus preoperative chemoradiotherapy, TME, and optional adjuvant chemotherapy in locally advanced rectal cancer (RAPIDO): a randomised, open-label, phase 3 trial. Lancet Oncol 2021; 22(1):29–42.

15. Wang X, Liu D, Zeng X, et al. Dual-energy CT quantitative parameters for evaluating immunohistochemical biomarkers of invasive breast cancer. Cancer Imaging 2021; 21(1):4.

16. Wu N, Cao QW, Wang CN, et al. Association between quantitative spectral CT parameters, Ki-67 expression, and invasiveness in lung adenocarcinoma manifesting as ground-glass nodules. Acta Radiol 2023; 64(4):1400–1409.

17. Chen XH, Ren K, Liang P, et al. Spectral computed tomography in advanced gastric cancer: can iodine concentration non-invasively assess angiogenesis? World J Gastroenterol 2017; 23(9):1666–1675.

18. Wang YL, Zhang HW, Mo YQ, et al. Application of dual-layer spectral detector computed tomography to evaluate the expression of Ki-67 in colorectal cancer. J Chin Med Assoc 2022; 85(5):610–616.

19. Gao W, Zhang Y, Dou Y, et al. Association between extramural vascular invasion and iodine quantification using dual-energy computed tomography of rectal cancer: a preliminary study. Eur J Radiol 2023; 158:110618.

20. Fan S, Li X, Zheng L, et al. Correlations between the iodine concentrations from dual energy computed tomography and molecular markers Ki-67 and HIF-1α in rectal cancer: a preliminary study. Eur J Radiol 2017; 96:109–114.

21. Malekzadeh Moghani M, Alahyari S, et al. Pathological predictors of response to neoadjuvant treatment in rectal carcinoma. J Gastrointest Cancer 2021; 52(2):690–695.

22. Sun Q, Liu T, Liu P, et al. Perineural and lymphovascular invasion predicts for poor prognosis in locally advanced rectal cancer after neoadjuvant chemoradiotherapy and surgery. J Cancer 2019; 10(10):2243–2249.

23. Chen YG, Chen MQ, Guo YY, et al. Apparent diffusion coefficient predicts pathology complete response of rectal cancer treated with neoadjuvant chemoradiotherapy. PLoS One 2016; 11(4):e0153944.

24. Yu J, Xu Q, Song JC, et al. The value of diffusion kurtosis magnetic resonance imaging for assessing treatment response of neoadjuvant chemoradiotherapy in locally advanced rectal cancer. Eur Radiol 2017; 27(5):1848–1857.

25. Bakke KM, Meltzer S, Grøvik E, et al. Sex differences and tumor blood flow from dynamic susceptibility contrast MRI are associated with treatment response after chemoradiation and long-term survival in rectal cancer. Radiology 2020; 297(2):352–360.

26. Ciolina M, Caruso D, De Santis D, et al. Dynamic contrast-enhanced magnetic resonance imaging in locally advanced rectal cancer: role of perfusion parameters in the assessment of response to treatment. Radiol Med 2019; 124(5):331–338.

27. Jain RK. Normalization of tumor vasculature: an emerging concept in antiangiogenic therapy. Science 2005; 307(5706):58–62.